

Spin injection in ferromagnet-semiconductor heterostructures at room temperature (invited)

Klaus H. Ploog^{a)}

Paul Drude Institute for Solid State Electronics, D-10117 Berlin, Germany

In this article we summarize our recent work on room-temperature spin injection in Fe/GaAs and MnAs/GaAs heterostructures. The most critical issue for injection of spin polarized electrons (holes) from the ferromagnet (FM) into the semiconductor (SC) is the control of the atomic arrangement at the FM/SC interface during molecular beam epitaxial growth of these rather dissimilar materials. For many years the formation of a magnetically dead layer at the Fe/GaAs interface has prevented spin injection. In addition to the accurate control of the FM/SC interface, the formation of a Schottky barrier between FM and SC for efficient spin injection via tunneling is the second critical issue for successful experiments. We describe in detail our approaches to solve these problems.

© 2002 American Institute of Physics. [DOI: 10.1063/1.1446125]

I. INTRODUCTION

The functionality of conventional semiconductor devices used in electronics and photonics relies on the precise control of transport and storage of electric charges. However, in addition to a well defined charge, electrons have a well defined spin of either $+1/2$ or $-1/2$ (angular momentum). The two allowed spin states could hence stand for the “zero” and “one” states in logical operations. Therefore, using not only the charge but also the spin of electrons to carry information in ferromagnet-semiconductor (FM-SC) hybrid structures makes feasible the development of novel functionalities in such spin-electronic (spintronic) devices with the prospects of higher speed and reduced power consumption.^{1,2}

The main obstacle to the practical realization of such spintronic devices has been the problem of electrically injection electrons with a controlled spin orientation into semiconductors at room temperature. The huge challenge for materials engineering is thus to monolithically integrate, e.g., by epitaxy or wafer bonding, suitable ferromagnets and semiconductors with well-defined heterointerfaces which allow efficient spin injection from the ferromagnetic layer into the semiconductor heterostructure. The most recently studied layer structures have unfortunately exhibited either a Curie temperature being far below room temperature (ternary $\text{Ga}_x\text{Mn}_x\text{As}$ on GaAs)³ or formed a nonmagnetic interfacial layer (Fe on GaAs)⁴ which prevented efficient spin injection. We have reinvestigated the growth of bcc Fe films on GaAs by molecular beam epitaxy (MBE)⁵ and we have studied MBE growth and properties of hexagonal binary MnAs films on GaAs(001).⁶ In this article we review our recent results on these two very different FM/SC heterostructures which are both ferromagnetic at room temperature and which allowed room-temperature injection of spin-polarized electrons into a (Ga,In)As light emitting diode (LED).⁷ by measuring the degree of the circular polarization of the emitted light resulting from the electron-hole recombination, we have obtained a direct measure of the spin polarization.

II. RESULTS AND DISCUSSION

A. Fe-on-GaAs

Certainly Fe-on-GaAs is one of the most widely studied epitaxial FM-SC hybrid systems. The stable bcc Fe phase with its bulk lattice constant being nearly half that of GaAs ($2a_{\text{Fe}}/a_{\text{GaAs}}=1.012$) grows epitaxially on GaAs(001) and GaAs(110) by MBE.^{8,9} Hence, GaAs seems to provide an almost ideal substrate for the epitaxy of Fe films, and the magnetic properties, including evolution of the magnetic order and the correlation between uniaxial stress and cubic magnetic anisotropy as a function of layer thickness, as well as the magnetic reversal process have been investigated in detail.^{10–12} Most of the observed properties were related to interfacial chemical reactions and to the atomic-scale nucleation processes, as monitored by electron diffraction and scanning tunneling microscopy (STM) for various Ga- and As-terminated surface reconstructions of the GaAs(001) substrate.^{12–14} However, when revisiting the Fe-on-GaAs systems⁵ we realized that in these previous studies little attention had been paid to the micron-scale surface morphology of the Fe-on-GaAs layers and to the existence of macroscopic defects which might strongly affect the local magnetic properties.

Our detailed study of MBE growth on bcc Fe films on GaAs(001) having different surface reconstructions as well as on GaAs(311)A, and (331)A revealed three major results.⁵ First, to avoid the formation of interfacial $\text{Fe}_x\text{Ga}_y\text{As}_z$ compounds, growth of the Fe films must be carried out in As-free environment on well-ordered GaAs surfaces at substrate temperatures as low as possible. Second, Fe growth on Ga-terminated surfaces which might reduce interface reactions leads inevitably to the formation of macroscopic defects, even though the overall rms roughness of 20-nm-Fe films can be below 1 nm. Third, due to the higher adatom mobility, growth of Fe on GaAs(311)A and (331)A is achieved at lower substrate temperature, i.e., even at 0 °C. This suppresses the formation of nonmagnetic interfacial layers more efficiently on As-terminated surfaces which are indispensable for the formation of smooth epitaxial Fe layers free of

^{a)}Electronic mail: ploog@pdi-berlin.de

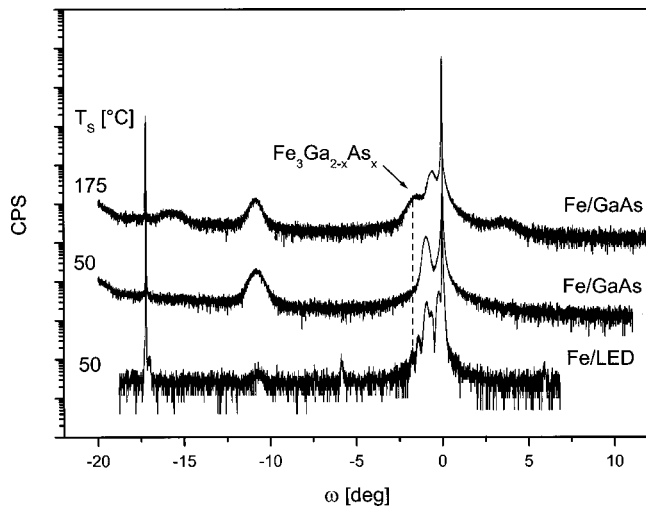


FIG. 1. Double-crystal XRD spectra from 20-nm-Fe films grown on As-stable (2×4) GaAs(001) by MBE at 175 and 50 °C, recorded between the symmetric GaAs(400) and (200) reflections. The lower trace is from the (Ga,In)As LED structure. The curves are vertically shifted for clarity.

macroscopic defects.^{5,15} The As-terminated GaAs surfaces minimize Fe–Ga exchange reactions which might generate the macroscopic defects.

Figure 1 shows the double-crystal x-ray diffraction spectra obtained from 20 nm Fe films grown on As-stable (2×4) GaAs(001) surfaces at different temperatures. The growth rate of Fe was 0.2 nm/min. The Fe/LED sample surface was protected by an Al cap layer, while the two Fe/GaAs samples were covered by a thin Ag layer. The important result is that no interfacial $Fe_xGa_yAs_z$ layer can be observed from the samples grown at 50 °C. The next obstacle affecting the experimental attempts to inject spin polarized electrons from Fe into GaAs came along with the theoretical considerations of Schmidt *et al.*¹⁶ who explained the negative results of previous experiments by the conductivity mismatch between the two materials. In the diffuse regime (i.e., ohmic contacts) the spin injection coefficient $\gamma \approx \sigma_{SC} / \sigma_{FM} \ll 1$. Fortunately, Rashba¹⁷ demonstrated shortly after that tunnel contacts can substantially increase the spin injection and solve the problem of mismatch in the conductivities of FM and SC. As a consequence, the Fe layer on our inverted *n-i-p* (Ga,In)As LED structure (inset, Fig. 2) forms a Schottky barrier,⁸ and we were able to detect the spin polarization of injected electrons by the circular polarization of electroluminescence.⁷

The active region of the MBE-grown LED (left-hand side inset of Fig. 2) is comprised of two 4-nm- $Ga_{0.8}In_{0.2}As$ quantum wells (QWs) separated by a 10-nm-GaAs barrier and sandwiched between two 50-nm-undoped GaAs spacer layers. On top of this intrinsic region, a 70-nm-*n*-doped GaAs layer was grown. The 20-nm-thick Fe injection layer was deposited on this *n*-GaAs in the attached As-free metal MBE chamber. Finally, the sample was capped with a 10-nm-Al protection layer. The electroluminescence (EL) measurements were carried out in Faraday geometry with the LED mounted in a superconducting magnet system. The EL signal was collected from the backside of the transparent substrate (Fig. 2, left inset). The circular polarization was

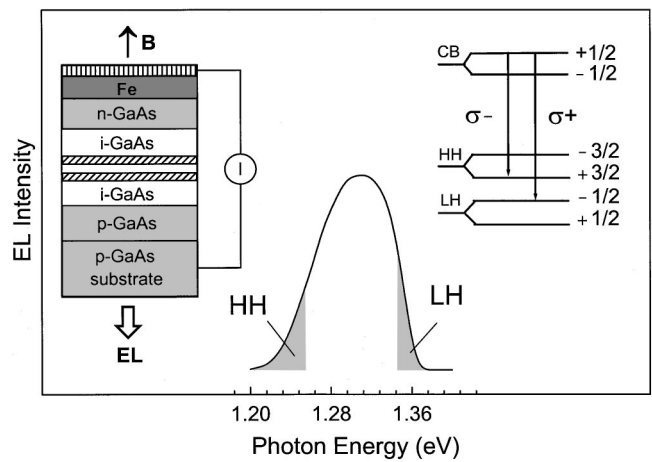


FIG. 2. EL spectrum recorded at 300 K. Left-hand side inset: device structure with directions of the magnetic field (B) and the emitted light (EL). Right-hand side inset: circular polarization of the EL light from recombination of electrons with spin +1/2.

analyzed by passing the EL light through a photoelastic modulator (PEM) and a linear polarizer. Thereby, the LED was operated with short current pulses locked to maximum or minimum phase shifts of the PEM.⁷

The EL spectrum of the LED at room temperature, shown in Fig. 2, reveals one peak at 1.3 eV in accordance with the design of the active region. The EL peak width of 90 meV is larger than the heavy-hole/light-hole splitting which enables us to analyze both heavy-hole and light-hole transitions separately. The intensity component $I_+(I_-)$ of right (left) circularly polarized light has been determined by integrating over the low- and high-energy part of the EL peak for the heavy- and light-hole contribution (shaded areas in Fig. 2). For a given polarization degree of injected electrons and unpolarized holes, we expect the same absolute value but opposite signs for the circular polarization of degree $P = (I_+ - I_-) / (I_+ + I_-)$ with its absolute value identical to the spin polarization of recombining electrons (right inset of Fig. 2). The polarization degree P is shown in Fig. 3 for heavy- and light-hole transitions as a function of an external mag-

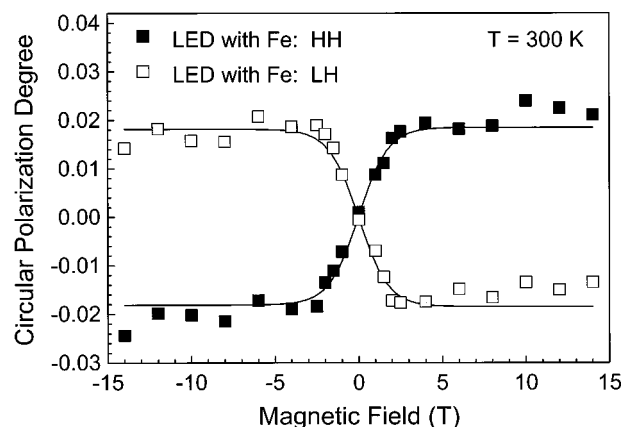


FIG. 3. Circular polarization degree P for heavy-hole (full squares) and light-hole (open squares) transitions vs external magnetic field. The Fe magnetization curve is shown in arbitrary units with two opposite signs (solid lines).

netic field B together with the out-of-plane magnetization of the Fe layer which was independently obtained by spontaneous Hall effect measurements.¹⁵ Both circular polarization curves follow in the whole magnetic field range the Fe magnetization and reveal the expected complementary behavior of P for heavy- and light-hole transitions. These room-temperature results provide clear evidence for the injection of spin polarized electrons from Fe into GaAs with an efficiency of 2%. The signatures of spin injection were not observed for the reference LED without Fe cap layer. An artifact due to polarization dependent reflection of the EL light at the Fe interface is excluded, since the reflection properties of Fe do not produce the complementary behavior found for the heavy- and light-hole transitions.

Our results demonstrate that our Fe layers deposited at low temperature on n -GaAs form Schottky-type contacts which give rise to tunneling under appropriate bias conditions. Hence, electrons from the Fe layer must tunnel through the Schottky barrier before reaching the active region of the LED. Such a tunneling process leads to an enhanced spin injection efficiency, as predicted¹⁷ since it is not affected by the resistance mismatch. This approach thus makes Fe a promising candidate as a tunneling spin injector paving the way for room-temperature operation of spintronics devices.

B. MnAs-on-GaAs

Hexagonal MnAs is ferromagnetic at room temperature, however, it undergoes several phase transitions upon cooling down from the growth temperature [about 250 °C for MnAs-on-GaAs(001)]. In Fig. 4 (top) we show schematically the epitaxial orientation of the semimetallic MnAs to GaAs as experimentally established:^{18,19} $(\bar{1}\bar{1}00)\text{MnAs}||(\text{001})\text{GaAs}$ and $[\text{0001}]\text{MnAs}||[\bar{1}\bar{1}0]\text{GaAs}$, i.e., the hexagonal prism plane is parallel to the cubic plane. This break of symmetry at the interface results in an asymmetric character of the interfacial structure and hence of the misfit parameters which depend strongly on the actual in-plane direction. The lattice misfit $f_0^{(1)}$ with respect to the GaAs $[\bar{1}\bar{1}0]$ direction, i.e., between MnAs $\{00.2\}$ and GaAs $\{110\}$ planes, amounts to more than 30%, while the $f_0^{(2)}$ value for the GaAs $[\text{110}]$ direction, i.e., between MnAs $\{1120\}$ and GaAs $\{110\}$ planes, reaches only about 7.5%.

We have directly monitored the formation of the MnAs-on-GaAs(001) interface during MBE *in situ* by combining reflection high-energy electron diffraction (RHEED) and reflection difference spectroscopy (RDS).¹⁹ The GaAs(001)- $c(4\times 4)$ surface reconstruction provides the As-rich template of choice for the growth of MnAs at $T_s = 250^\circ\text{C}$ with a rather low rate of 20 nm/h and a high As_4/Mn BEP ratio of 90. The epitaxial orientation of the MnAs films with respect to the substrate, as determined by RHEED and HRTEM, is type A, i.e., $\text{MnAs}(\bar{1}\bar{1}00)||\text{GaAs}(001)$ and $\text{MnAs}[\text{0001}]\|\text{GaAs}[\bar{1}\bar{1}0]$ (see Fig. 4). The surface topography of 100 nm MnAs films, as imaged by AFM, exhibits flat regular furrows along MnAs $[\text{0001}]$ with a depth of 4–7 nm and a width of 100–200 nm. The rms roughness of a $10\ \mu\text{m}^2$ scan amounts to about 1 nm which is a very reasonable value.

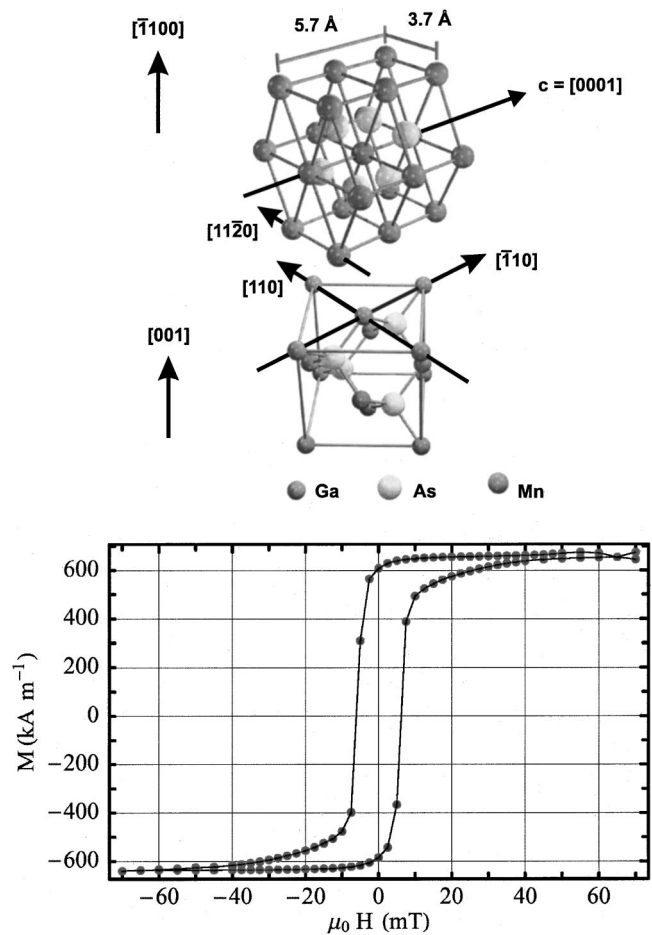


FIG. 4. Top: epitaxial relationship between $\text{MnAs}(\bar{1}\bar{1}00)$ and $\text{GaAs}(001)$. The c axis of the hexagonal MnAs unit cell lies in the growth plane. The epitaxial orientation of the MnAs film as shown here is of type A, i.e., $\text{MnAs}(1100)||\text{GaAs}(001)$ and $\text{MnAs}[\text{0001}]\|\text{GaAs}[\text{110}]$. Bottom: magnetization M of a 100-nm-thick MnAs film measured as a function of applied magnetic field along MnAs $[\text{1120}]$, i.e., the easy axis of magnetization.

Magnetization measurements with the magnetic field applied in-plane along MnAs $[\text{1120}]$, the easy axis of magnetization, yield a nearly perfect square hysteresis loop at room temperature, as shown in Fig. 4 (bottom).⁶ The measured saturation magnetic moment of $2.58\ \mu_B/\text{Mn}$ atom at 60 mT is even higher than the bulk value, due to the improved crystal quality of the epitaxial MnAs layers. The existence of magnetic domains in these MnAs epilayers has been studied by high resolution magnetic force microscopy. This detailed investigation has revealed new insights into the correlation between epilayer topography and magnetic domain structures.⁶

In MnAs-on-GaAs(001) the large dependence of lattice misfit on direction leads to an unusual anisotropy of the misfit accommodation process.^{20,21} Due to the length limitation, we will discuss only the case of the large misfit $f_0^{(1)}$. The HRTEM image in Fig. 5(a) reveals the nature of the interface along GaAs $[\text{110}]$ where the lattice mismatch is above 30%. The HRTEM contrast of the MnAs lattice imaged along $[\text{1120}]$ is wavy-like with a period corresponding to the hexagonal lattice constant $c = 0.57\ \text{nm}$ as confirmed by image simulations. Due to the different interference pattern of both materials, the atomically abrupt interface can be seen very

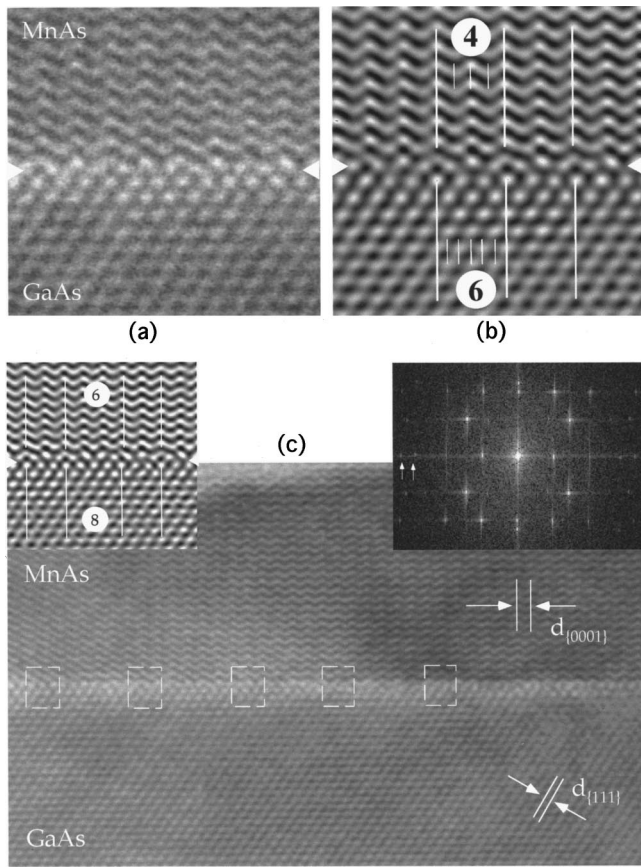


FIG. 5. (a) Cross-sectional HRTEM image of MnAs/GaAs(001) interface in MnAs[1120]||GaAs[110] projection and (b) corresponding Fourier-filtered image. The atom positions correspond to the dark regions of the image, (c) large-area HRTEM image of MnAs/GaAs(001) interface in the same projection as in (a). Insets: magnified and Fourier-filtered part of interface image showing the secondary defect (left-hand side) and Fourier spectrum of the total image (right-hand side).

clearly. Any localized misfit dislocations are not visible in the HRTEM image, as expected for incoherent systems. In fact, the interface does not look completely incoherent, even though the interfacial MnAs/GaAs bond strength is weaker than in pure III–V heterostructures. A detailed analysis of the interface structures reveals that the lattice misfit is accommodated by forming a coincidence lattice [Fig. 5(b)]. Every fourth MnAs{0002} plane fits every sixth GaAs{220} plane resulting in a commensurate-like interfacial region. Beyond this, no coherence strain with a coincidence lattice unit is detectable at this stage, except for the distortions in the first MnAs layer next to the interface.

This 4/6-ratio of the coincidence lattice reduces the natural lattice misfit to a value of about 5%. This large deviation $F_0 = (ma_S - na_E)/ma_S$ (m, n positive integers; a_S, a_E lattice spacings of substrate and epilayer) must be accompanied by secondary or coincidence-lattice misfit dislocations in order to guarantee epitaxial growth. As shown in Fig. 5(c) (inset) such defects are indeed observed at the interface, and they are characterized by an additional {0001} plane in one coincidence mesh, extending its ratio to 8/6. The measured average spacing of these secondary dislocations at every third unit (Fig. 4) is sufficient to relieve the coincidence lattice misfit, due to $F_0 = (14d_{\{0002\}} - 20d_{\{220\}}) = -0.0008$. There is

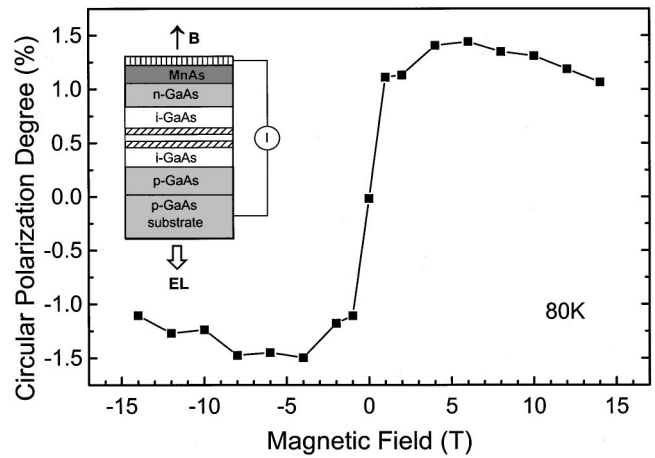


FIG. 6. Difference of circular polarization degree P as a function of external magnetic field measured at 80 K from LEDs with and without MnAs cap layer. Inset: schematic layer sequence of LED depicting the directions of magnetic field B and emitted light EL . (Ga,In)As QWs are indicated by hatched areas.

thus no residual elastic strain detectable in the [0001] direction. In perfect agreement, the spacing of the diffraction spots in the Fourier spectrum of Fig. 5(c) (inset) fits to strain-free bulk values. The overall result is an interface structure with commensurate domains having a perfect coincidence lattice arrangement separated by a network of secondary defects.^{20,21}

It should be pointed out here that the low misfit direction is probably responsible for the epitaxial alignment. The described unique interface structure along [0001] is thus more the result of an epitaxial constraint rather than the primary driving force for it. Nevertheless, the perfect adjustment of the atoms in a coincidence lattice during interface formation demonstrates the basic tendency that this structure corresponds to a low-energy interface configuration.

The electrical spin injection from MnAs into GaAs was again studied by means of the circular polarization of EL from an inverted $n-i-p$ (Ga,In)As LED in the same configuration as described for the Fe-on-GaAs system.²² The polarization degree P measured at 80 K shown in Fig. 6 for heavy-hole transitions as a function of an external magnetic field B . These results provide evidence for the injection of spin polarized electrons from MnAs into GaAs with an efficiency of 1.5% at 80 K (and slightly lower efficient at 300 K). These signatures of spin injection are absent in the reference samples without MnAs cap layer. The semimetallic MnAs also forms Schottky-type contacts on GaAs(001). However, the asymmetry of this specific interface and the differences of the (unknown) thermal expansion coefficients will certainly affect the actual injection process of spin polarized electrons.

III. CONCLUSION

We have demonstrated spin injection from two ferromagnetic metals into a semiconductor with efficiencies of about 2% up to room temperature. The injection mechanism is understood in terms of a tunneling process through a Schottky barrier. In this context it is noteworthy that experi-

mental evidence for spin-polarized electron tunneling using a scanning tunneling microscope was reported almost a decade ago²³ and very recently.²⁴

Finally, as mentioned above, the polarization degree P for transitions involving only one type of hole is identical to the spin polarization of recombining electrons in the (Ga,In)As QWs. However, if the spin relaxation time τ_S ^{25,26} in the quantum well is considerably shorter than the radiative carrier lifetime τ_R , the measured value of P would be a lower limit for the spin polarization of injected electrons, i.e., the pin injection efficiency for our experiments would then be larger than 2% by a factor of about τ_R/τ_S . Measurements of the crucial time constants τ_R and τ_S for our LED structures are underway in our laboratory. Further optimization of the ferromagnet–semiconductor interface as well as the device structure will lead to larger efficiencies.

ACKNOWLEDGMENTS

The author wishes to thank his colleagues L. Däweritz, H. Kostial, M. Ramsteiner, F. Schippan, H.-P. Schönherr, A. Trampert, and H. J. Zhu for their active contributions to this work. Part of the work was sponsored by the Bundesministerium für Bildung und Forschung.

¹S. Datta and B. Das, Appl. Phys. Lett. **56**, 665 (1990).

²G. A. Prinz, Phys. Today **48**, 58 (1995).

³Y. Ohno, D. K. Young, B. Beschoten, F. Matsukara, H. Ohno, and D. D. Awschalom, Nature (London) **402**, 790 (1999).

⁴Y. B. Xu, E. T. M. Kernohan, D. J. Freeland, A. Ercole, M. Tselepi, and J. A. C. Bland, Phys. Rev. B **58**, 890 (1998).

⁵H.-P. Schönherr, R. Nötzel, W. Q. Ma, and K. H. Ploog, J. Appl. Phys. **89**, 169 (2001).

⁶F. Schippan, G. Behme, L. Däweritz, K. H. Ploog, B. Dennis, K. U. Neumann, and K. R. A. Ziebeck, J. Appl. Phys. **88**, 2766 (2000).

⁷H. J. Zhu, M. Ramsteiner, H. Kostial, M. Wassermeier, H.-P. Schönherr, and K. H. Ploog, Phys. Rev. Lett. **87**, 016601 (2001).

⁸J. R. Waldrop and R. W. Grant, Appl. Phys. Lett. **34**, 630 (1979).

⁹G. A. Prinz and J. J. Krebs, Appl. Phys. Lett. **39**, 397 (1981).

¹⁰J. M. Florczak and E. D. Dahlberg, Phys. Rev. B **44**, 4338 (1991).

¹¹C. Daboo, R. J. Hicken, E. Gu, M. Gester, S. J. Gray, D. E. P. Eley, E. Ahmad, J. A. C. Bland, R. Ploessl, and J. N. Chapman, Phys. Rev. B **51**, 15964 (1995).

¹²P. M. Thibado, E. Kneeder, B. T. Jonker, R. R. Bennett, B. V. Shanabrook, and L. J. Whitman, Phys. Rev. B **53**, R10481 (1996).

¹³E. M. Kneeder, B. T. Jonker, P. M. Thibado, R. J. Wagner, B. V. Shanabrook, and L. J. Whitman, Phys. Rev. B **56**, 8163 (1997).

¹⁴M. Gester, C. Daboo, H. J. Hicken, S. J. Gray, A. Ercole, and J. A. C. Bland, J. Appl. Phys. **80**, 347 (1996).

¹⁵K. J. Friedland, R. Nötzel, H.-P. Schönherr, A. Riedel, H. Kostial, and K. H. Ploog, Physica E (Amsterdam) **10**, 442 (2001).

¹⁶G. Schmidt, D. Ferrand, L. W. Molenkamp, A. T. Filip, and B. J. van Wees, Phys. Rev. B **62**, R4790 (2000).

¹⁷E. I. Rashba, Phys. Rev. B **62**, R16267 (2000).

¹⁸M. Tanaka, Mater. Sci. Eng., B **31**, 117 (1995).

¹⁹F. Schippan, A. Trampert, L. Däweritz, and K. H. Ploog, J. Vac. Sci. Technol. B **17**, 1716 (1999).

²⁰A. Trampert, F. Schippan, L. Däweritz, and K. H. Ploog, Inst. Phys. Conf. Ser. **164**, 305 (1999).

²¹A. Trampert and K. H. Ploog, Cryst. Res. Technol. **35**, 793 (2000).

²²M. Ramsteiner *et al.* (unpublished).

²³S. F. Alvarado and P. Renaud, Phys. Rev. Lett. **68**, 1387 (1992).

²⁴V. LaBella, D. W. Bullock, Z. Ding, C. Emery, A. Venkatesan, W. F. Oliver, G. J. Salamo, P. M. Thibado, and M. Mortazavi, Science **292**, 1518 (2001).

²⁵D. Hägele, M. Oestreich, W. W. Rühle, N. Nestle, and K. Eberl, Appl. Phys. Lett. **73**, 1580 (1998).

²⁶A. Malinowski, R. S. Britton, T. Grevatt, R. T. Harley, D. A. Ritchie, and Y. Simmons, Phys. Rev. B **62**, 13034 (2000).